SPECKLE FILTERING FOR JERS-1/SAR IMAGERY

Masatoshi MORI, Tomonori YOKOYAMA†, and Noboru YAMAMOTO†

Department of Management Engineering, Kinki University, Iizuka City 820, Japan
†Graduate School of Advanced Technology, Kinki University,
Iizuka City 820, Japan

ABSTRACT:

Synthetic Aperture Radar (SAR) images by JERS-1 are enhanced by reducing speckle noise. The Gamma MAP filter by Lopes et al. has been applied to ERS-1/SAR or C-SAR images, and they successfully obtained the speckle reduced images. The speckle is reduced as a function of the coefficient of variation within a local window in the Gamma MAP filter, in which the threshold values are used to classify pixels. The theoretical estimate of the thresholds by the Gamma MAP filtering algorithm for JERS-1/SAR images is quite different from the estimate by the present analysis of the distribution of the coefficient of variation for 1-look, 2-look, and 3-look processes. These thresholds for JERS-1/SAR images are determined based on the distribution of the observed local coefficient of variation within a window. SAR images with good quality are obtained by the present method of estimating the thresholds.

1. INTRODUCTION

First Synthetic Aperture Radar (SAR) images by satellite sensors had been obtained by Seasat for Earth observation by NASA. However, the active interval of observation was short due to a satellite malfunction.

Now, a massive number of SAR images have been acquired by ERS-1/SAR and JERS-1/SAR sensors. The only defect of these SAR images is coherent noise known as speckle noise. So SAR images are granular in quality, and are especially remarkable in homogeneous areas such as agricultural areas. To date, many researches have been performed to reduce speckle noise (Touzi, 1988; Lopes, 1990). Adaptive speckle filters to preserve radiometric and textural information in SAR images have been developed by Lopes et al. (Nezry, 1991; Lopes, 1993), which were recently refined, culminating in the Gamma MAP (Maximum A Posteriori) filter.

Two thresholds in discriminating between a homogeneous class and a heterogeneous class within a local window were introduced in the Gamma MAP filter. The operation in that filter is performed depending on the coefficient of variation. Many SAR images of ERS-1 with high quality are obtained by use of the Gamma MAP filter. Two threshold values are, however, not so easy or clear to determine.

2. MODEL FOR SAR IMAGES

Speckle noise is uniformly distributed on SAR images, so the value of the observed intensity includes both the true signal value from a target and the speckle noise with random process. This multiplicative model (Lopes, 1993) is formalized as follows:

$$I(t) = S(t) \cdot N(t) \qquad (1)$$

where $I(t)$ is the observed intensity at the position t on an image, $S(t)$ is the true signal value, and $N(t)$ is the noise intensity with random process, respectively. A texture in images within a homogeneous or heterogeneous class is characterized as a function of the coefficient of variation $C_I(t_0)$ within a local window, which is defined as

$$C_I(t_0) = \sigma_I / \bar{I}(t_0) \qquad (2)$$

where σ_I is a standard deviation of $I(t)$ within the window, $\bar{I}(t_0)$ is a mean of $I(t)$, and t_0 is the central position of the window.

The filter operation for SAR images is performed depending on the value of $C_I(t_0)$. Regions with a small $C_I(t_0)$, such as agricultural areas, are considered to be in the homogeneous class. On the other hand, the regions with a large $C_I(t_0)$ may contain edge or linear features. Thus, the operation in filtering is defined based on two threshold values, C_N and C_{max}, where C_N is the speckle coefficient of variation, which is defined as

$$C_N = \sigma_N / \bar{N} \qquad (3)$$

where σ_N is the standard deviation of the noise, and $\bar{N}$ is the mean of the noise.

The other threshold is C_{max}. To estimate the original signal by comparing $C_I(t_0)$ with these two threshold values, the following procedures (Lopes, 1993) are obtained:

i) $C_I(t_0) \leq C_N$: $\hat{S}(t_0) = \bar{I}(t_0)$.
ii) $C_N < C_I(t_0) \leq C_{max}$: the previous filter operated.
iii) $C_{max} < C_I(t_0)$: $\hat{S}(t_0) = I(t_0)$.

where $\hat{S}(t_0)$ is the estimated value of the original signal at position t_0. In the case of i), a standard smoothing procedure is applied to the local window, where the area is considered to be in the homogeneous class. In the case of ii), the previous well-known filter is operated within the window. The estimated signal obtained using Kuan filter (Kuan, 1985), for examples, is given as follows:

$$\hat{S}(t_0) = I(t_0) \cdot W(t_0) + \bar{I}(t_0) \cdot (1 - W(t_0)) \quad (4)$$

$$W(t_0) = [1 - C_N^2/C_I^2(t_0)]/(1 + C_N^2) \quad (5)$$

In the present report, we used the Kuan filter for the case of ii). In the case of iii), the existence of structures such as an edge or linear feature is considered within the window, in which such smoothing procedures reduce the quality of the images. So the observed value is adopted as the estimated signal value.

3. THRESHOLDS FOR JERS-1/SAR

In the algorithm of the Gamma MAP filter, the speckle coefficient of variation is estimated as $C_N = 1/\sqrt{L}$ for the L-look multiplicative scheme. If speckle noise is assumed to be a random process, then $\bar{N} = 1$ and $\sigma_N = 1/L$. This result means that $C_N = 1$ for 1-look of SAR images. Figure 1 shows the histograms of counts of the coefficient of variation of a 5×5 window within a homogeneous area of 1-look (a), 2-look (b), and 3-look (c) JERS-1/SAR images (2116 pixels), respectively.

In such a homogeneous area, the coefficient of variation is considered to be similar to the speckle coefficient of variation, which is distributed around C_N. So we adopted a mean value of the distribution of the coefficient of variation as C_N. The mean value 0.513 of the coefficient of variation of a 1-look image in Fig. 1(a) is, however, rather different from the theoretical estimate $C_N = 1$. Also, the mean values of 0.361 and 0.284 are different from the theoretical estimates of $C_N=0.707$ and 0.577 for 2-look and 3-look images, respectively.

In addition to C_N, C_{max} is estimated in the Gamma MAP filter as

$$C_{max} = \sqrt{2}C_N \quad (6)$$

C_{max} is 1.414, 1.000, and 0.816 for 1-look, 2-look, and 3-look images, respectively. To estimate C_{max}, we analyzed the distribution of the coefficient of variation of Fig. 1. The distribution can be assumed to be a Gaussian distribution. A χ^2-test of fitness for a Gaussian distribution is performed to the observed distribution. The results of a χ^2-test with 5% level shows that the observed distribution is judged to be Gaussian. We estimate $C_{max} = C_N + 1.645\sigma_N$, where σ_N is a standard deviation of the distribution of the coefficient of variation. Thus we obtained the results of $C_{max}=0.64$, 0.44, and 0.37 for 1-look, 2-look, and 3-look images from Fig. 1(a), (b), (c). These results are shown in Table 1.

Table 1. Comparison of the thresholds.

thresholds		Gamma MAP filter	the present estimate
C_N	(1-look)	1.000	0.513
C_N	(2-look)	0.707	0.361
C_N	(3-look)	0.577	0.284
C_{max}	(1-look)	1.414	0.64
C_{max}	(2-look)	1.000	0.44
C_{max}	(3-look)	0.816	0.37

This discrepancy between the theoretical estimate and the observed one comes from the probability density function of the speckle process and is assumed to be a Gamma distribution (Lopes, 1993). However, the observed distribution of $C_I(t_0)$ in a homogeneous area, as shown in Fig. 1, is quite similar to a Gaussian distribution.

4. RESULTS

Figure 2(a) shows an original 1-look image of 1024×1024 pixels of JERS-1/SAR by NASDA, which is obtained after being processed from the raw data (path:65, row:241, 1992/01/23, level 0). This image is of Mt. Fuji in Japan. Also, Fig. 3(a) shows a 3-look image of the same scene as in Fig. 2(a). The speckle noise is more remarkable in homogeneous areas of Fig. 2(a) than that of Fig. 3(a). On the other hand, the spacital resolution is higher in Fig. 2(a) than in Fig. 3(a). Thus, although the speckle noise of SAR images could be reduced by multi-look processing, the spatial resolution decreases simultaneously. The speckle reduction techniques by keeping the spatial resolution higher are expected so far.

Figure 2(b) shows the speckle reduction filtered 1-look image obtained from Fig. 2(a) by use of $C_N=0.513$ and $C_{max}=0.64$ in Table 1. The speckle in Fig. 2(b) is effectively reduced, particularly in the homogeneous
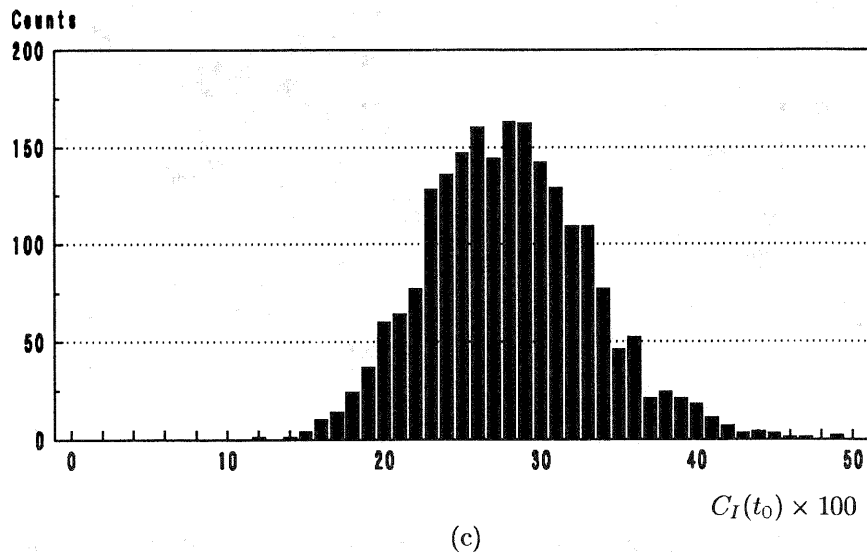
262

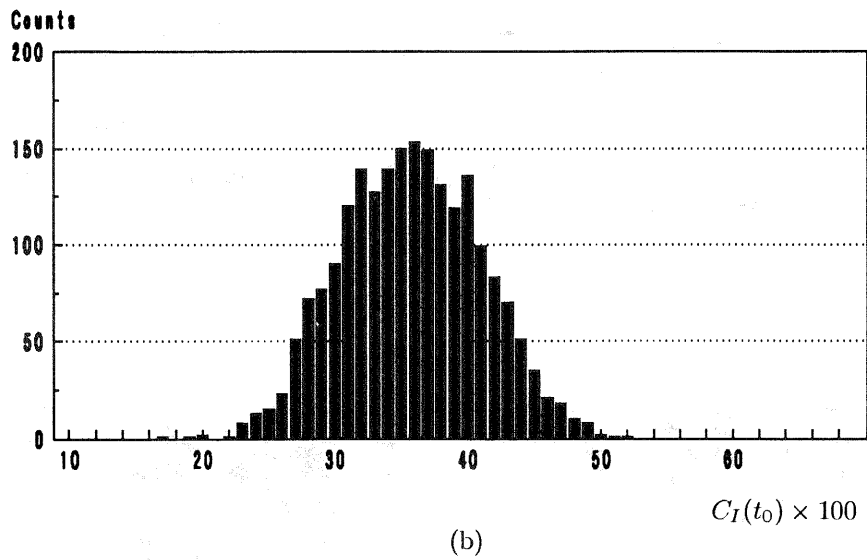International Archives of Photogrammetry and Remote Sensing. Vol. XXXI, Part B2. Vienna 1996
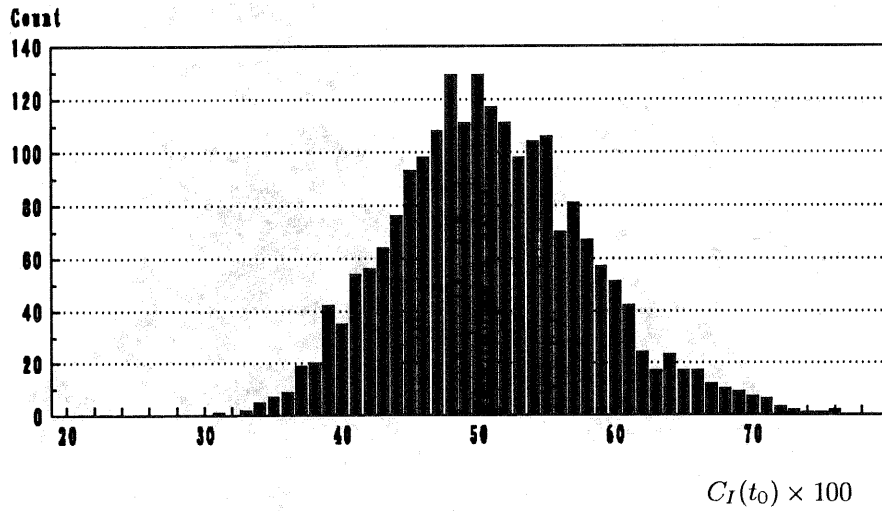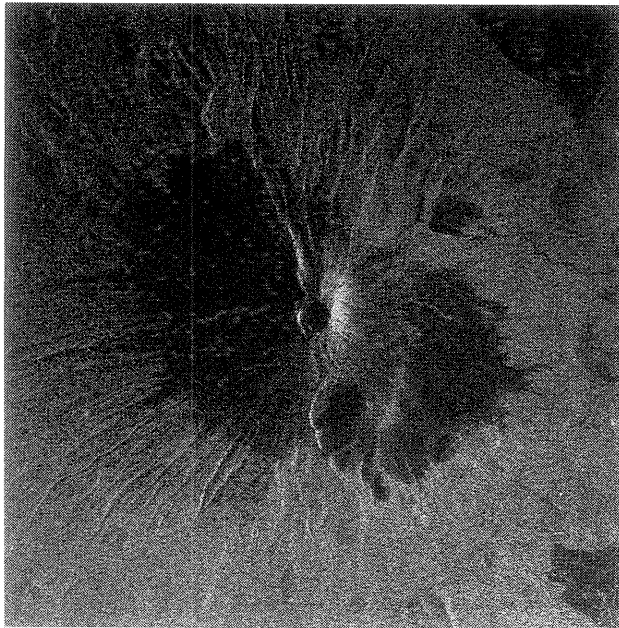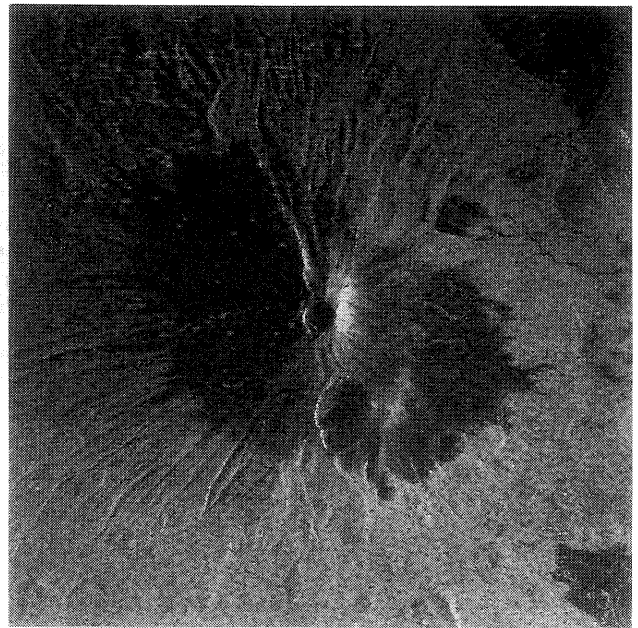
(a)

(b)

(c)

Figure 1. Distributions of the observed local coefficient of variation within a homogeneous area (2116 pixels) for 1-look (a), 2-look (b), and 3-look images of JERS-1/SAR, respectively.

263

International Archives of Photogrammetry and Remote Sensing. Vol. XXXI, Part B2. Vienna 1996
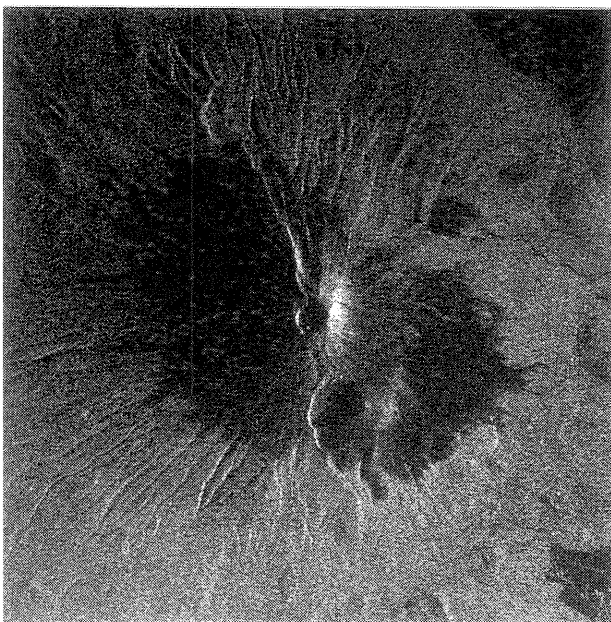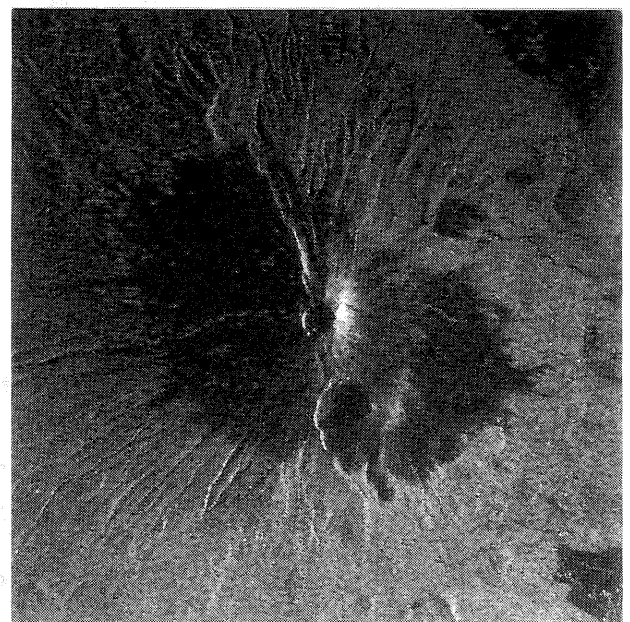
(a)   (b)

Figure 2. 1-look images of Mt. Fuji (Japan) by JERS-1/SAR. (a) an original image; (b) a filtered
image by use of the present estimate as the thresholds.

(a)   (b)

Figure 3. 3-look images of Mt. Fuji (Japan) by JERS-1/SAR. (a) an original image; (b) a filtered
image by use of the present estimate as the thresholds.

264

International Archives of Photogrammetry and Remote Sensing. Vol. XXXI, Part B2. Vienna 1996

regions, and the edge lines of boundaries are still preserved. By the use of C_N and C_{max} in the Gamma MAP filter, the image becomes unclear due to the over smoothing effect. The theoretical estimates C_N and C_{max} are apparently higher compared with Fig. 1. The filtered 3-look image shown in Fig. 3(b) was also obtained by the same algorithm as that in Fig. 2(b). Though the speckle in the image is reduced, the spatial resolution is reduced as compared with the 1-look image.

5. CONCLUSIONS

The two thresholds of C_N and C_{max} in reducing speckle for 1-look, 2-look, and 3-look of JERS-1/SAR images have been estimated for the first time in the present report. Then, the filtered images of 1-look, 2-look, and 3-look processes by use of these thresholds were obtained and the speckle was successfully reduced. The thresholds estimated from the Gamma MAP filter have been applied to ERS-1/SAR and C-SAR images so far.

The theoretical estimates of the thresholds for JESR-1/SAR images are apparently high. The discrepancy between the theoretical and the observed estimates for JERS-1/SAR may be due to the assumption of the Gamma MAP filtering. The speckle and the radar reflectivity are both assumed to be a Gamma distribution in the Gamma MAP filter. However, the distribution of the coefficient of variation $C_I(t)$ of JERS-1/SAR could be estimated as a Gaussian distribtion from Fig. 1(a), (b).

7. REFERENCES

Kuan, D.T., Sawchuk, A.A., Strand, T.C., and Chavel, P., 1985, Adaptive noise smoothing filter for images with signal-dependent noise, IEEE Trans. Pattern Anal. Machine Intell., Vol.PAMI-7, pp.165-177.

Lopes, A., Touzi, R., and Nezry, E., 1990, Adaptive Speckle Filters and Scene Heterogeneity, IEEE Trans. Geosci. Remote Sensing, Vol.GE-28, No.6, pp.992-1000.

Lopes, A., Nezry, E., Touzi, R., and Laur, H., 1993, Structure Detection and Statistical Adaptive Speckle Filtering in SAR Images, Int. J. Remote Sensing, Vol.14, No.9, pp.1735-1758.

Nezry, E., Lopes, A. and Touzi, R., 1991, Detection of Structural and Textural Features for SAR Images Filtering, Proceedings of IGARSS '91, pp.2169-2172.

Touzi, R., Lopes, A. and Bousquest, P., 1988, A Statistical and Geometrical Edge Detector for SAR Images, IEEE Trans. Geosci. Remote Sensing, Vol.GE-26, pp.764-773.

265